

From Claringbullite to a New Spin Liquid Candidate $\text{Cu}_3\text{Zn}(\text{OH})_6\text{FCl}$ *

Zili Feng(冯子力)^{1,2†}, Wei Yi(衣玮)^{3†}, Kejia Zhu(朱恪嘉)¹, Yuan Wei(魏源)^{1,2}, Shanshan Miao(苗杉杉)¹,
 Jie Ma(马杰)^{4,5}, Jianlin Luo(雒建林)^{1,2,6}, Shiliang Li(李世亮)^{1,2,6**},
 Zi Yang Meng(孟子杨)^{1,7,8**}, Youguo Shi(石友国)^{1,2**}

¹Beijing National Laboratory of Condensed Matter Physics, and Institute of Physics, Chinese Academy of Sciences, Beijing 100190

²School of Physical Sciences, University of Chinese Academy of Sciences, Beijing 100190

³Nano Electronics Device Materials group, National Institute for Materials Science (NIMS), 1-1 Namiki, Tsukuba, Ibaraki 305-0044, Japan

⁴Key Laboratory of Artificial Structures and Quantum Control, School of Physics and Astronomy, Shanghai Jiao Tong University, Shanghai 200240

⁵Collaborative Innovation Center of Advanced Microstructures, Nanjing 210093

⁶Collaborative Innovation Center of Quantum Matter, Beijing 100190

⁷CAS Center of Excellence in Topological Quantum Computation and School of Physical Sciences, University of Chinese Academy of Sciences, Beijing 100190

⁸Songshan Lake Materials Laboratory, Dongguan 523808

(Received 16 November 2018)

The search for quantum spin liquid (QSL) materials has attracted significant attention in the field of condensed matter physics in recent years, however so far only a handful of them are considered as candidates hosting QSL ground state. Owing to their geometrically frustrated structures, Kagome materials are ideal systems to realize QSL. We synthesize the kagome structured material claringbullite ($\text{Cu}_4(\text{OH})_6\text{FCl}$) and then replace inter-layer Cu with Zn to form $\text{Cu}_3\text{Zn}(\text{OH})_6\text{FCl}$. Comprehensive measurements reveal that doping Zn^{2+} ions transforms magnetically ordered $\text{Cu}_4(\text{OH})_6\text{FCl}$ into a non-magnetic QSL candidate $\text{Cu}_3\text{Zn}(\text{OH})_6\text{FCl}$. Therefore, the successful syntheses of $\text{Cu}_4(\text{OH})_6\text{FCl}$ and $\text{Cu}_3\text{Zn}(\text{OH})_6\text{FCl}$ provide not only a new platform for the study of QSL but also a novel pathway of investigating the transition between QSL and magnetically ordered systems.

PACS: 75.10.Kt, 75.40.Cx, 67.30.er

DOI: 10.1088/0256-307X/36/1/017502

In recent years, the search for quantum spin liquid (QSL) materials, usually realized in frustrated magnets, has attracted great interests due to the exotic anyonic excitations therein as well as their potential relationship with quantum computation and unconventional superconductivity.^[1–6] The commonly searched ground states for QSL are frustrated magnets with honeycomb, triangular and kagome structures. Kagome Heisenberg antiferromagnet is a promising direction for the pursuit of QSL ground states. Although several kagome materials are proposed to host QSL ground states, the detailed nature of these QSL candidates still needs further intensive investigations to verify.^[7–12]

Among the discovered kagome Heisenberg antiferromagnetic QSL candidates,^[10,13,14] herbertsmithite $\text{ZnCu}_3(\text{OH})_6\text{Cl}_2$ ^[7,9,15–17] and Zn-doped Barlowite $\text{Cu}_3\text{Zn}(\text{OH})_6\text{FBr}$ ^[10–12,18–21] are the two well-known kagome QSL materials. In particular, the high-quality single crystal of herbertsmithite provides the rare opportunity to explicitly reveal the detailed momentum-frequency dependence of the magnetic spectra in inelastic neutron scattering exper-

iment, in which the spinon continuum manifest.^[7] Meanwhile, many related materials are also studied, such as $\text{Cu}_3\text{Mg}(\text{OH})_6\text{Cl}_2$, $\text{Cu}_3\text{Cd}(\text{OH})_6\text{SO}_4$, $\text{Y}_3\text{Cu}_9(\text{OH})_{19}\text{Cl}_8$ and $\text{YCu}_3(\text{OH})_6\text{Cl}_3$.^[22–27] To synthesize a promising kagome QSL material, the perfect kagome structure must retain intact and the inter-layer interaction shall be reduced, to optimize the perfect frustration in the 2D plane in order to suppress any magnetic order. Unfortunately, most materials develop magnetic order at low temperatures, which is usually accompanied by structure distortion that breaks the perfect kagome lattice geometry.

In this work, we successfully synthesize a new kagome Heisenberg antiferromagnetic QSL candidate, $\text{Cu}_3\text{Zn}(\text{OH})_6\text{FCl}$ and its parent compound $\text{Cu}_4(\text{OH})_6\text{FCl}$ (claringbullite). X-ray diffraction (XRD) shows pure $\text{Cu}_3\text{Zn}(\text{OH})_6\text{FCl}$ is synthesized and chemical analysis show that the content of Zn^{2+} ions in the inter-kagome plane is about 0.7 per formula unit. Although some Cu^{2+} ions remain in the inter-kagome plane, structure analysis reveals that the perfect kagome plane is preserved and thermodynamic measurements show that magnetic order is completely

*Supported by the National Key Research and Development Program (2016YFA0300502, 2017YFA0302901, 2016YFA0300604 and 2016YFA0300501), the Strategic Priority Research Program of the Chinese Academy of Sciences (XDB28000000, XDB07020100 and QYZDB-SSW-SLH043), the National Natural Science Foundation of China under Grant Nos 11421092, 11574359, 11674370, 11774399, 11474330 and U1732154.

†Zili Feng and Wei Yi contributed to this work equally.

**Corresponding authors. Email: slli@iphy.ac.cn; zymeng@iphy.ac.cn; ygshi@iphy.ac.cn

© 2019 Chinese Physical Society and IOP Publishing Ltd

suppressed in $\text{Cu}_3\text{Zn}(\text{OH})_6\text{FCl}$. Moreover, our AC magnetic susceptibility (ACMS) measurements also exclude spin glass behavior in $\text{Cu}_3\text{Zn}(\text{OH})_6\text{FCl}$, which is found in other putative QSL candidates.^[28] All these evidences suggest that $\text{Cu}_3\text{Zn}(\text{OH})_6\text{FCl}$ is a new QSL candidate. On the other hand, claringbullite develops magnetic order below 15 K. The evolution from $\text{Cu}_4(\text{OH})_6\text{FCl}$ to $\text{Cu}_3\text{Zn}(\text{OH})_6\text{FCl}$, therefore, provides an ideal occasion to investigate the transition between magnetically ordered states and QSL, in which theoretically expected dynamical signatures of fractionalized anyonic excitations^[29–31] and other exotic properties of the associated \mathbb{Z}_2 topologically ordered QSLs^[32,33] could be experimentally revealed in future.

$\text{Cu}_4(\text{OH})_6\text{FCl}$ and $\text{Cu}_3\text{Zn}(\text{OH})_6\text{FCl}$ were synthesized using the hydrothermal method. For $\text{Cu}_4(\text{OH})_6\text{FCl}$, about 0.55 g $\text{Cu}_2(\text{OH})_2\text{CO}_3$ (Alfa Aeser), 0.43 g $\text{CuCl}_2 \cdot 2\text{H}_2\text{O}$ (Alfa Aeser), 0.185 g NH_4F (Alfa Aeser) and 0.1 g concentrated hydrochloric acid (HCl, mass fraction about 35%) were mixed with about 20 mL deionized water in a 25 mL vessel. For $\text{Cu}_3\text{Zn}(\text{OH})_6\text{FCl}$, about 0.5 g $\text{Cu}_2(\text{OH})_2\text{CO}_3$, 0.38 g $\text{ZnCl}_2 \cdot 4\text{H}_2\text{O}$ (Alfa Aeser), 0.095 g NH_4F and 0.1 g HCl were also mixed with about 20 mL deionized water in a 25 mL vessel. The samples both were heated at 200°C for one day and then slowly cooled to room temperature. Green powder were collected by washing and drying the production.

Table 1. Structure parameters of $\text{Cu}_3\text{Zn}(\text{OH})_6\text{FCl}$ at room temperature. The space group is $P6_3/mmc$ (No. 194). $Z = 2$, $a = b = 6.65377(11) \text{ \AA}$, $c = 9.18896(11) \text{ \AA}$, and $V = 352.3166 \text{ \AA}^3$. The occupancy of Zn site is 0.319 and the others are 1 according to a splitting model.^[34,35] The R indexes are $R_{\text{wp}} = 4.583\%$ and $R_p = 3.259\%$.

Site	w	x	y	z	B
Cu	6g	0.5	0	0	1.794(31)
Zn	2d	1/3	2/3	3/4	2.290(117)
Cl	2c	2/3	1/3	3/4	1.336(112)
F	2b	0.0	0.0	3/4	1.767(125)
O	12k	0.20076	0.79924(24)	0.90986(27)	0.112(89)
H	12k	0.12472	0.87528	0.86683	2.265

$\text{Cu}_3\text{Zn}(\text{OH})_6\text{FCl}$ was characterized by powder XRD and no impurity peaks were found. The measured XRD data and the calculated pattern, refined by the Rietveld method using the program RIETAN-FP^[36], are plotted in Fig. 1(a). The refined structure parameters are listed in Table 1. The XRD measurement was performed at room temperature on a Rigaku Smartlab high-resolution diffractometer using $\text{Cu K}\alpha_1$ radiation ($\lambda = 1.5406 \text{ \AA}$). Two forms of chemical component analyses were used to determine the Zn content. First, energy-dispersive X-ray spectra were measured on a Hitachi S-4800 scanning electron microscope at an accelerating voltage of 15 kV, with an accumulation time of 90 s. Then, inductively coupled plasma atomic emission spectroscopy was performed using a Thermo IRIS Intrepid II instrument. These results show that the stoichiometric ratio of Cu and

Zn ions is about 3:0.7.

The sample was pressed and cut into pieces about 1 mm^2 to perform the thermodynamic measurements. The magnetization data were measured using a superconducting quantum interference device magnetometer (Quantum Design MPMS). The specific heat data were measured in a physical property measurement system (PPMS) at zero magnetic field between 2 K and 30 K and the specific heat below 2 K was measured using a He-3 system.

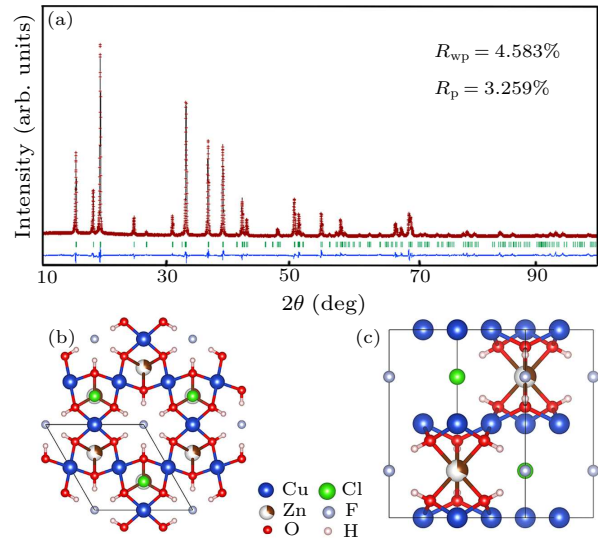


Fig. 1. XRD pattern and structure of $\text{Cu}_3\text{Zn}(\text{OH})_6\text{FCl}$. (a) Powder XRD data and Rietveld refinement profile of $\text{Cu}_3\text{Zn}(\text{OH})_6\text{FCl}$. (b) Top view (ab plane) of the structure of $\text{Cu}_3\text{Zn}(\text{OH})_6\text{FCl}$. (c) Slide view of the structure of $\text{Cu}_3\text{Zn}(\text{OH})_6\text{FCl}$.

$\text{Cu}_3\text{Zn}(\text{OH})_6\text{FCl}$ crystallized in hexagonal lattice with space group $P6_3/mmc$ (No. 194). The lattice parameters are $a = b = 6.65377(11) \text{ \AA}$, $c = 9.18896(11) \text{ \AA}$. As shown in Fig. 1, $\text{Cu}_3\text{Zn}(\text{OH})_6\text{FCl}$ has a perfect kagome lattice at room temperature. The kagome planes show AA stacking and are separated by Zn^{2+} ions. Table 1 provides the detailed structure parameters of $\text{Cu}_3\text{Zn}(\text{OH})_6\text{FCl}$. In $\text{Cu}_4(\text{OH})_6\text{FCl}$, the interlayer Cu^{2+} ions split from the equilibrium sites and shows three equivalent positions,^[35] while in $\text{Cu}_3\text{Zn}(\text{OH})_6\text{FCl}$, the interlayer Zn^{2+} ions sit at the center of the triangle of the kagome Cu layer.

Figure 2(a) shows the temperature dependence of magnetic moment of $\text{Cu}_3\text{Zn}(\text{OH})_6\text{FCl}$ and $\text{Cu}_4(\text{OH})_6\text{FCl}$ at 1 kOe below 50 K. The vertical coordination is in logarithmic scale to highlight the salient difference. The moment of $\text{Cu}_4(\text{OH})_6\text{FCl}$ increases abruptly at about 17 K, which is its magnetic phase transition temperature as reported in the previous study,^[35] while $\text{Cu}_3\text{Zn}(\text{OH})_6\text{FCl}$ shows no obvious magnetic order transition down to 2 K. Furthermore, the ACMS measurements at zero magnetic field show no frequency dependence down to 2 K, as shown in Fig. 2(b), which suggests no spin-glass

behavior.^[28] The $1/\chi$ data between 300 K and 2 K of $\text{Cu}_3\text{Zn}(\text{OH})_6\text{FCl}$ at 10 kOe in zero-field-cooling (ZFC) and field-cooling (FC) conditions are shown in the inset of Fig. 2(a). The Curie–Weiss law $\chi = c/(T - \theta_{\text{CW}})$ was used to fit the data between 150 K and 300 K and gave $\theta_{\text{CW}} = -223$ K. The value of θ_{CW} (19.2 meV) indicates a strong antiferromagnetic interaction between Cu^{2+} ions in the kagome layer, suggesting strong frustration in the system. The Curie constant is $1.556 \text{ K}\cdot\text{emu}\cdot\text{mol}^{-1}$. Assuming $S = 1/2$ and using the typical g factor value in kagome lattice for Cu ions, i.e., $g = 2.3 \pm 0.1$,^[34,10] the Cu content can be calculated to be 3.28 ± 0.14 per formula unit. This gives that Zn content is 0.72 ± 0.14 per formula unit, which is consistent with the chemical analysis discussed above.

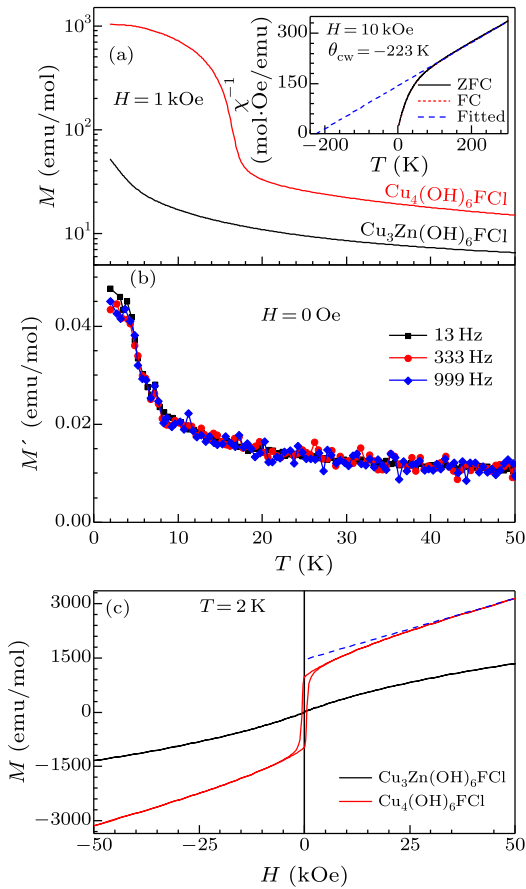


Fig. 2. Magnetic properties of $\text{Cu}_3\text{Zn}(\text{OH})_6\text{FCl}$ and $\text{Cu}_4(\text{OH})_6\text{FCl}$. (a) Temperature dependence of magnetic moment between 2 K and 50 K at 1 kOe for $\text{Cu}_3\text{Zn}(\text{OH})_6\text{FCl}$ and $\text{Cu}_4(\text{OH})_6\text{FCl}$. Inset: zero-field-cooling and field-cooling $1/\chi$ at 10 kOe for $\text{Cu}_3\text{Zn}(\text{OH})_6\text{FCl}$. Curie–Weiss fitting (blue dashed line) gives the Curie temperature $\theta_{\text{CW}} = -223$ K. (b) The temperature dependence of the real component of ACMS for $\text{Cu}_3\text{Zn}(\text{OH})_6\text{FCl}$. These data were measured under zero magnetic field and the peak amplitude of applied excitation field was 1 Oe. (c) Field dependence of magnetic moment of $\text{Cu}_3\text{Zn}(\text{OH})_6\text{FCl}$ and $\text{Cu}_4(\text{OH})_6\text{FCl}$ at 2 K. The blue dashed line is linear fitting ($M = A + B \times H$) of high field magnetization for $\text{Cu}_4(\text{OH})_6\text{FCl}$.

Figure 2(c) shows the field dependence of magnetization of $\text{Cu}_3\text{Zn}(\text{OH})_6\text{FCl}$ and $\text{Cu}_4(\text{OH})_6\text{FCl}$ at 2 K.

$\text{Cu}_4(\text{OH})_6\text{FCl}$ shows obvious ferromagnetic behavior with the magnetization jump about $0.0865 \mu_B/\text{Cu}$, while $\text{Cu}_3\text{Zn}(\text{OH})_6\text{FCl}$ shows no visible hysteresis. The comparison between $\text{Cu}_4(\text{OH})_6\text{FCl}$ and $\text{Cu}_3\text{Zn}(\text{OH})_6\text{FCl}$ in Fig. 2(c) demonstrates the disappearance of magnetic order in the latter, although the Zn content is not equal to 1. A linear function $M = A + B \times H$ is used to fit the magnetization at high field as shown in Fig. 2(c). Similar fitting analysis has been performed in $\text{Cu}_{4-x}\text{Zn}_x(\text{OH})_6\text{FBr}$ and the Zn content dependence (doping dependence) of $B(x)$ has been obtained in Fig. 6(b) in Ref. [12]. Compared with the fitting results in Fig. 2(c), here we find a very consistent value in the x -dependence of the Zn content. For $\text{Cu}_4(\text{OH})_6\text{FCl}$, we obtain $B = 0.035 \text{ emu}\cdot\text{mol}^{-1}$, almost the same as that in $\text{Cu}_4(\text{OH})_6\text{FBr}$; and for $\text{Cu}_3\text{Zn}(\text{OH})_6\text{FCl}$, we obtain $B = 0.02 \text{ emu}\cdot\text{mol}^{-1}$, this value is very close to the $x = 0.7$ value in $\text{Cu}_{4-x}\text{Zn}_x(\text{OH})_6\text{FBr}$, again suggesting the success of synthesizes of $\text{Cu}_3\text{Zn}(\text{OH})_6\text{FCl}$, which may be a new QSL candidate.

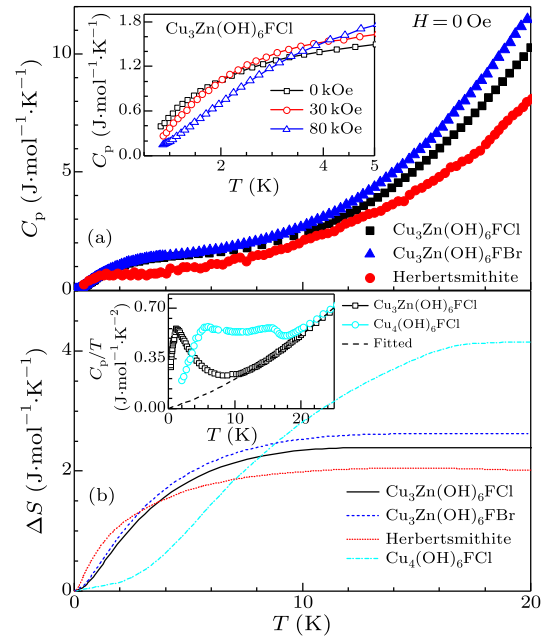


Fig. 3. Thermal dynamic properties of $\text{Cu}_3\text{Zn}(\text{OH})_6\text{FCl}$, $\text{Cu}_3\text{Zn}(\text{OH})_6\text{FBr}$, herbertsmithite, and $\text{Cu}_4(\text{OH})_6\text{FCl}$. (a) Specific heat at zero magnetic field over temperature for $\text{Cu}_3\text{Zn}(\text{OH})_6\text{FBr}$ (blue), $\text{Cu}_3\text{Zn}(\text{OH})_6\text{FCl}$ (black), and herbertsmithite (red). The data of $\text{Cu}_3\text{Zn}(\text{OH})_6\text{FBr}$ was taken from Fig. 2(c) in Ref. [10] and that of herbertsmithite was from Fig. 3(a) in Ref. [34]. The inset plots the low temperatures behavior of $\text{Cu}_3\text{Zn}(\text{OH})_6\text{FCl}$ at 0 Oe, 30 kOe and 80 kOe. (b) Magnetic entropy of $\text{Cu}_3\text{Zn}(\text{OH})_6\text{FCl}$, $\text{Cu}_3\text{Zn}(\text{OH})_6\text{FBr}$, herbertsmithite and $\text{Cu}_4(\text{OH})_6\text{FCl}$. The inset shows the specific heat over temperature at zero field below 25 K of $\text{Cu}_3\text{Zn}(\text{OH})_6\text{FCl}$ and $\text{Cu}_4(\text{OH})_6\text{FCl}$. The dashed line is background contribution of $\text{Cu}_3\text{Zn}(\text{OH})_6\text{FCl}$ fitted using $C_{\text{bg}} = aT^2 + bT^3$.

Similar contrasts have also been reported in detail in comparison in the Zn-doped $\text{Cu}_{4-x}\text{Zn}_x(\text{OH})_6\text{Cl}_2$, which shows hysteresis and QSL candidate herbertsmithite $\text{Cu}_3\text{Zn}(\text{OH})_6\text{Cl}_2$,^[37] as well as the more re-

cent Zn-doped barlowite $\text{Cu}_{4-x}\text{Zn}_x(\text{OH})_6\text{FBr}$ and the QSL candidate $\text{Cu}_3\text{Zn}(\text{OH})_6\text{FBr}$.^[12] Such consistency further reaffirms that all these three kagome material families, $\text{Cu}_{4-x}\text{Zn}_x(\text{OH})_6\text{Cl}_2$, $\text{Cu}_{4-x}\text{Zn}_x(\text{OH})_6\text{FBr}$ and $\text{Cu}_{4-x}\text{Zn}(\text{OH})_x\text{FCl}$, are ideal platforms of achieving kagome QSL with $x \rightarrow 1$. Moreover, our results are consistent with a previous study on $\text{Cu}_4(\text{OH})_6\text{FCl}$, in which a magnetic transition at around 15 K was reported.^[35] Recent neutron scattering and NMR studies reveal that $\text{Cu}_4(\text{OH})_6\text{FBr}$ change its structure at low temperature,^[12,20] and such structural change gives rise to magnetic order. It is possible that a similar process can happen in $\text{Cu}_4(\text{OH})_6\text{FCl}$ as well. Further neutron scattering experiment, similar to that performed on $\text{Cu}_4(\text{OH})_6\text{FBr}$,^[11,12] will reveal this process.

Figure 3(a) shows the specific heat of $\text{Cu}_3\text{Zn}(\text{OH})_6\text{FCl}$ at zero field from 0.8 K to 20 K. For comparison, the data of $\text{Cu}_3\text{Zn}(\text{OH})_6\text{FBr}$ (from Fig. 2(c) in Ref. [10]) and herbertsmithite (from Fig. 3(a) in Ref. [34]) were also plotted. These three compounds show similar behavior at low temperatures. Especially, $\text{Cu}_3\text{Zn}(\text{OH})_6\text{FCl}$ and $\text{Cu}_3\text{Zn}(\text{OH})_6\text{FBr}$ nearly coincide below 10 K. The inset shows the specific heat of $\text{Cu}_3\text{Zn}(\text{OH})_6\text{FCl}$ below 5 K at different fields and no magnetic order was observed. For $\text{Cu}_4(\text{OH})_6\text{FCl}$, the magnetic order transition arises at about 15 ~ 17 K, which is manifested by the high-temperature peak of C_p/T shown in the inset of Fig. 3(b). With further decrease of the temperature, C_p/T of $\text{Cu}_4(\text{OH})_6\text{FCl}$ shows another peak at 5 K, and C_p/T of $\text{Cu}_3\text{Zn}(\text{OH})_6\text{FCl}$ shows a peak at around 3 K. These low-temperature peaks have also been seen in $\text{Cu}_{4-x}\text{Zn}_x(\text{OH})_6\text{FBr}$ ^[12,19] and in the previous studies of $\text{Cu}_4(\text{OH})_6\text{FCl}$ ^[35] as well as in herbertsmithite.^[13,37,38] They are all significantly affected by magnetic field, as exemplified in the inset of Fig. 3(a) for $\text{Cu}_3\text{Zn}(\text{OH})_6\text{FCl}$ and the inset of Fig. 2(c) for $\text{Cu}_3\text{Zn}(\text{OH})_6\text{FBr}$ in Ref. [10]. The current understanding of such behavior is that these are the contribution from inter kagome layer Cu ions,^[10,12,17] which have very weak interactions among themselves and are easily polarized by external field.

One can obtain some information of kagome QSL from the current data by subtracting the background contribution using the formula $C_{\text{bg}} = aT^2 + bT^3$. This formula was used to fit the specific heat data between 20 K and 30 K in zero field for $\text{Cu}_3\text{Zn}(\text{OH})_6\text{FCl}$, $\text{Cu}_4(\text{OH})_6\text{FBr}$, herbertsmithite, and $\text{Cu}_4(\text{OH})_6\text{FCl}$. The dashed line in the inset of Fig. 3(b) shows the fitted data for $\text{Cu}_3\text{Zn}(\text{OH})_6\text{FCl}$. The T^2 term comes from the spin correlations above 20 K in the two-dimensional structure and the T^3 term, on the other hand, comes from the three-dimensional lattice contribution.^[34] Figure 3(b) shows the magnetic entropies of $\text{Cu}_3\text{Zn}(\text{OH})_6\text{FCl}$, $\text{Cu}_3\text{Zn}(\text{OH})_6\text{FBr}$, herbertsmithite and $\text{Cu}_4(\text{OH})_6\text{FCl}$. At about 20 K, their magnetic entropies reach the corresponding maximal

values. The entropy of $\text{Cu}_3\text{Zn}(\text{OH})_6\text{FCl}$ lays between the values of $\text{Cu}_3\text{Zn}(\text{OH})_6\text{FBr}$ and herbertsmithite, while for $\text{Cu}_4(\text{OH})_6\text{FCl}$, its magnetic entropy is very close to that of $\text{Cu}_4(\text{OH})_6\text{FBr}$.^[12] These results indicate that $\text{Cu}_3\text{Zn}(\text{OH})_6\text{FCl}$ is a QSL candidate.

In summary, we have successfully synthesized a new QSL candidate material $\text{Cu}_3\text{Zn}(\text{OH})_6\text{FCl}$ and its parent material claringbullite $\text{Cu}_4(\text{OH})_6\text{FCl}$, and have performed comprehensive thermodynamic measurements on them. It is found that $\text{Cu}_3\text{Zn}(\text{OH})_6\text{FCl}$ is a highly frustrated kagome material, does not show magnetic order down to 0.8 K and hence is a good candidate for kagome QSL, whereas $\text{Cu}_4(\text{OH})_6\text{FCl}$ is magnetically ordered below 17 K. The possible structural change in $\text{Cu}_4(\text{OH})_6\text{FCl}$ accompanied with the development of magnetic order is worth being revealed by elastic neutron scattering. Our results consistently reveal the similarity of the three by now established families of the kagome Heisenberg antiferromagnets, $\text{Cu}_{4-x}\text{Zn}_x(\text{OH})_6\text{Cl}_2$, $\text{Cu}_{4-x}\text{Zn}_x(\text{OH})_6\text{FBr}$ and $\text{Cu}_{4-x}\text{Zn}(\text{OH})_x\text{FCl}$. As $x \rightarrow 1$, Heisenberg kagome QSL properties of $\text{Cu}_3\text{Zn}(\text{OH})_6\text{FCl}$ are similar to those of herbertsmithite $\text{Cu}_3\text{Zn}(\text{OH})_6\text{Cl}_2$ ^[13] and Zn-doped Barlowite $\text{Cu}_3\text{Zn}(\text{OH})_6\text{FBr}$.^[10]

Looking into the future, the pathway from $\text{Cu}_4(\text{OH})_6\text{FCl}$ to $\text{Cu}_3\text{Zn}(\text{OH})_6\text{FCl}$ offers the opportunity to investigate the transition between magnetically ordered systems to QSL states. Such investigations will have a very significant theoretical impact. As the material realization of Z_2 topological order, neutron scattering experiments on the possible kagome QSL in $\text{Cu}_3\text{Zn}(\text{OH})_6\text{FCl}$ and its transition to the magnetic order claringbullite $\text{Cu}_4(\text{OH})_6\text{FCl}$ could help to reveal the dynamical signature of the fractionalized anyonic excitations in the QSL ground state, as proposed by theoretical calculations in the vicinity of the QSL to magnetic order phase transition.^[30,31] In this regard, the materials such as $\text{Cu}_4(\text{OH})_6\text{FCl}$ and $\text{Cu}_3\text{Zn}(\text{OH})_6\text{FCl}$ presented in this work will greatly encourage the further theoretical and experimental developments of the new paradigms of quantum matter.

References

- [1] Anderson P W 1987 *Science* **235** 1196
- [2] Kitaev A Y 2003 *Ann. Phys.* **303** 2
- [3] Kitaev A and Preskill J 2006 *Phys. Rev. Lett.* **96** 110404
- [4] Balents L 2010 *Nature* **464** 199
- [5] Savary L and Balents L 2017 *Rep. Prog. Phys.* **80** 016502
- [6] Zhou Y, Kanoda K and Ng T 2017 *Rev. Mod. Phys.* **89** 025003
- [7] Han T H, Helton J S, Chu S, Nocera D, Rodriguez-Rivera J A, Broholm C and Lee Y S 2012 *Nature* **492** 406
- [8] Fu M X, Imai T, Han T H and Lee Y 2015 *Science* **350** 655
- [9] Norman M R 2016 *Rev. Mod. Phys.* **88** 041002
- [10] Feng Z L, Li Z, Meng X, Yi W, Wei Y, Zhang J, Wang Y, Jiang W, Liu Z, Li S and Meng Z Y 2017 *Chin. Phys. Lett.* **34** 077502
- [11] Wei Y, Feng Z, Lohstroh W, dela Cruz C, Yi W, Ding Z F, Zhang J, Tan C, Shu L and Wang Y C et al 2017 *arXiv:1710.02991* [cond-mat.str-el]

- [12] Feng Z, Wei Y, Liu R, Yan D, Wang Y C, Luo J, Senyshyn A, Cruz C d, Yi W, Mei J W, Meng Z Y, Shi Y and Li S 2018 *Phys. Rev. B* **98** 155127
- [13] Han T H, Helton J S, Chu S, Prodi A, Singh D K, Mazzoli C, Müller P, Nocera D G and Lee Y S 2011 *Phys. Rev. B* **83** 100402
- [14] Zheng J, Ran K, Li T, Wang J, Wang P, Liu B, Liu Z X, Norm, B, Wen J and Yu W 2017 *Phys. Rev. Lett.* **119** 227208
- [15] Imai T, Nytko E A, Bartlett B M, Shores M P and Nocera D G 2008 *Phys. Rev. Lett.* **100** 077203
- [16] Imai T, Fu M, Han T H and Lee Y S 2011 *Phys. Rev. B* **84** 020411
- [17] Han T H, Norman M R, Wen J J, Rodriguez-Rivera J A, Helton J S, Broholm C and Lee Y S 2016 *Phys. Rev. B* **94** 060409
- [18] Wen X G 2017 *Chin. Phys. Lett.* **34** 090101
- [19] Smaha R W, He W, Sheckelton J P, Wen J and Lee Y S 2018 *J. Solid State Chem.* **268** 123
- [20] Ranjith K M, Klein C, Tsirlin A A, Rosner H, Krellner C and Baenitz M 2018 *Sci. Rep.* **8** 10851
- [21] Pasco C M, Trump B A, Tran T T, Kelly Z A, Hoffmann C, Heinmaa I, Stern R and McQueen T M 2018 *Phys. Rev. Mater.* **2** 044406
- [22] Shores M P, Nytko E A, Bartlett B M and Nocera D G 2005 *J. Am. Chem. Soc.* **127** 13462
- [23] Colman R, Sinclair A and Wills A 2011 *Chem. Mater.* **23** 1811
- [24] Iqbal Y, Jeschke H O, Reuther J, Valentí R, Mazin I I, Greiter M, Thomale R 2015 *Phys. Rev. B* **92** 220404
- [25] Pustogow A, Li Y, Voloshenko I, Puphal P, Krellner C, Mzin I I, Dressel M and Valenti R 2017 *Phys. Rev. B* **96** 241114(R)
- [26] Puphal P, Bolte M, Sheptyakov D, Pustogow A, Kliemt K, Dtesel M, Baenitz M and Krellner C 2017 *J. Mater. Chem. C* **5** 2629
- [27] Sun W, Huang Y X, Nokhrin S, Pan Y and Mi J X 2016 *J. Mater. Chem. C* **4** 8772
- [28] Ma Z, Wang J, Dong Z Y, Zhang J, Li S, Zheng S H, Yu Y, Wang W, Che L, Ran K, Bao S, Cai Z, Čermák P, Schneidewind A, Yano S, Gardner J S, Lu X, Yu S L, Liu J M, Li S, Li J X and Wen J 2018 *Phys. Rev. Lett.* **120** 087201
- [29] Mei J W and Wen X G 2015 arXiv:1507.03007 [cond-mat.str-el]
- [30] Sun G Y, Wang Y C, Fang C, Qi Y, Cheng M and Meng Z Y 2018 *Phys. Rev. Lett.* **121** 077201
- [31] Becker J and Wessel S 2018 *Phys. Rev. Lett.* **121** 077202
- [32] Wen X G 1991 *Phys. Rev. B* **44** 2664
- [33] Wen X G 2017 *Rev. Mod. Phys.* **89** 041004
- [34] Han T, Singleton J and Schlueter J A 2014 *Phys. Rev. Lett.* **113** 227203
- [35] Yue X Y, Ouyang Z W, Wang J F, Xia Z C and He Z Z 2018 *Phys. Rev. B* **97** 054417
- [36] Rietveld H M 1969 *J. Appl. Crystallogr.* **2** 65
- [37] de Vries M A, Kamenev K V, Kockelmann W A, Sanchez-Benitez J and Harrison A 2008 *Phys. Rev. Lett.* **100** 157205
- [38] Helton J, Matan K, Shores M, Nytko E, Bartlett B, Yoshida Y, Takano Y, Suslov A, Qiu Y, Chung J H, Nocera D G and Lee Y S 2007 *Phys. Rev. Lett.* **98** 107204